

Convex and concave micro-structured silicone controls the shape, but not the polarization state of human macrophages

Electronic supplementary information

A. Materials & Methods Supplementary Data

Cell metabolic activity was reported as % reduction of alamarBlue and calculated with the flowing equation:

$$\% \text{ reduction of alamarBlue} = \frac{S_{AB}^x - S_{AB}^{\text{control}}}{S_{AB}^{100\% \text{ reduced}} - S_{AB}^{\text{control}}}$$

where S_{AB}^x is the alamarBlue fluorescence signal of the sample x , $S_{AB}^{100\% \text{ reduced}}$ is the signal of the 100% reduced form of alamarBlue and S_{AB}^{control} is the signal from the control: the culture medium supplemented with 10% (v/v) alamarBlue dye in the absence of cells. The 100% reduced form of alamarBlue was produced by autoclaving culture medium supplemented with 10% (v/v) alamarBlue at 121 °C for 15 min. The results were corrected for cell number and normalized to the activity of cells cultured on glass in basal medium.

Table S1 Morphometric descriptors quantified from the digitalized microscopic images of macrophages labelled with CellMask™.

Descriptor	Definition
Area	Contiguous area of each cell.
Aspect ratio (AR)	Ratio between the length of the major and minor axis of object-equivalent ellipse. Increasing values indicate increasingly elongated shape.
Circularity	A value of 1.0 indicates a perfect circle and less than one a starfish footprint or elongated shapes.
Feret Angle	Angle between the Feret's diameter (the longest distance between any two points on an object boundary), and a line parallel to the x-axis of the image.

Table S2 Primer sequences used for qRT-PCR.

Gene	Forward (5'-3')	Reverse (5'-3')	length (base pair)
GAPDH	AGTCAGCCGCATCTTCTTTT	CCAATACGACCAAATCCGTTG	97
TNF- α	CCGTCTCTACCAGACCAAG	CTGAGTCGGTCACCCTTCTC	148
IL-10	ACATCAAGGCGCATGTGAAC	CAGGGAAGAAATCGATGACAGC	95
CXCL10	CAGTCTCAGCACCATGAATCAA	CAGTTCTAGAGAGAGGTACTCCTTG	95

CCL22	GCGTGGTGTGCTAACCTTC	CCACGGTCATCAGAGTAGGC	115
CD197	GTGGTTTTACCGCCAGAGA	CACTGTGGTGTGTCTCCGA	142
CD206	GCTACCCCTGCTCCTGGTTT	CGCAGCGCTTGTGATCTCA	101

B. Endotoxin testing

Endotoxins are large molecules found in the cell wall of most gram-negative bacteria that are recognised by different cells of the immune system, including macrophages. Macrophage interaction with endotoxins results in an up-regulation of pro-inflammatory cytokines, notably TNF- α . Surface contamination with endotoxins can therefore lead to misleading conclusions in macrophages *in vitro* studies. To confirm the absence of significant endotoxin contamination, we performed parallel stimulations in the presence of polymyxin B, an antibiotic that binds and inactivates endotoxin^{1,2}. Flat PDMS samples as well as TCP control wells were seeded with THP-1 monocytes as described for morphometric analysis but 5 $\mu\text{g}/\text{mL}$ polymyxin B was added to half of the samples. On day three, three different concentrations of LPS (1 ng/mL, 10 ng/mL and 100 ng/mL) were added to wells containing polymyxin B and polymyxin B-free cultures. Samples with LPS served as positive controls. Additionally, pure medium was used as negative reference value. After 24h stimulation, the medium was harvested and tested for the presence of TNF- α using an ELISA kit (Ready SET-Go![®] ELISA Kit, e Bioscience) according to the manufacture's instruction.

Polymyxin B markedly suppressed TNF production induced by LPS in macrophages cultured in TCP but did not affect the already decreased TNF production of macrophages cultured in planar PDMS (Figure S1), confirming that endotoxin contamination is not a significant confounding factor in this study.

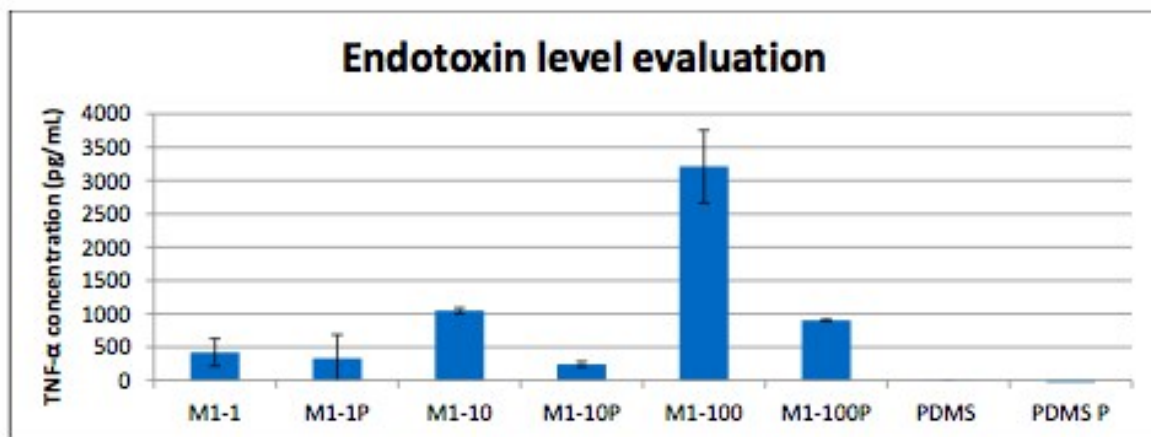


Figure 1 THP-1 macrophages were cultured on TCP or planar PDMS in the presence (P) or absence the endotoxin inhibitor Polymyxin B (5 $\mu\text{g}/\text{mL}$) for 3 days. Macrophages cultured on TCP were then stimulated with different concentrations of LPS (1 ng/mL in M1-1 and M1-1P, 10 ng/mL in M1-10 and M1-10P or 100 ng/mL in M1-100 and M1-100P) for 24h. TNF- α levels in culture supernatants were measured by ELISA. Values are the mean and standard deviation of triplicate cultures.

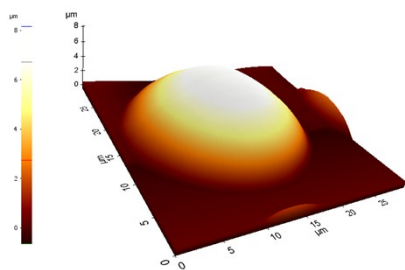
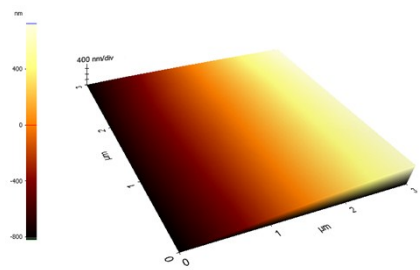
C. Surface characterization

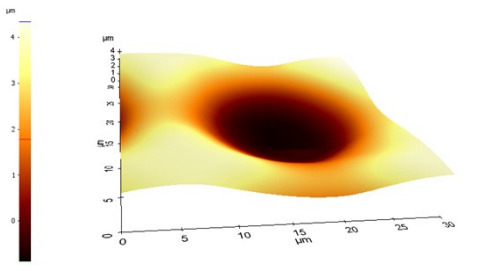
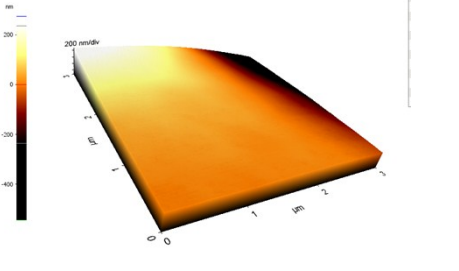
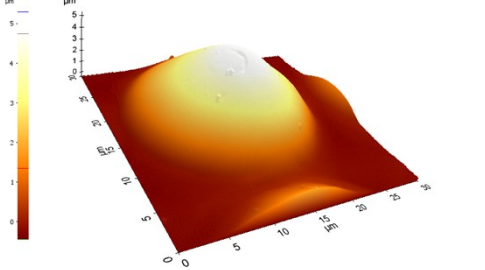
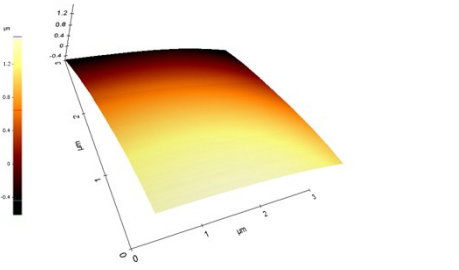
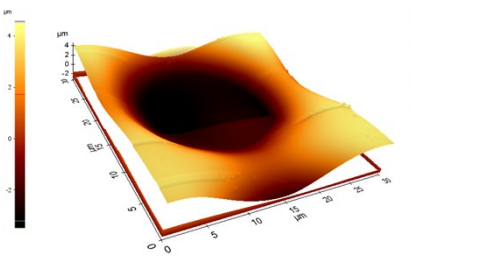
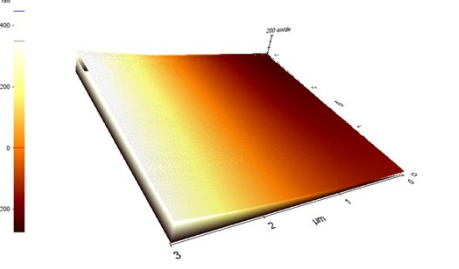
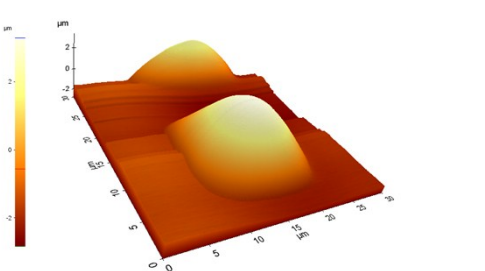
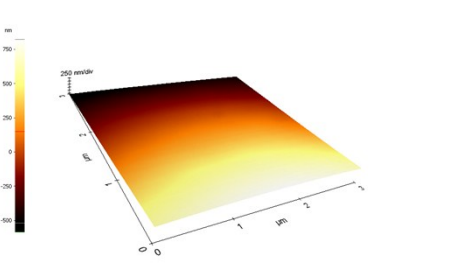
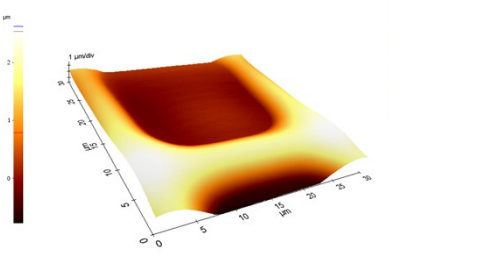
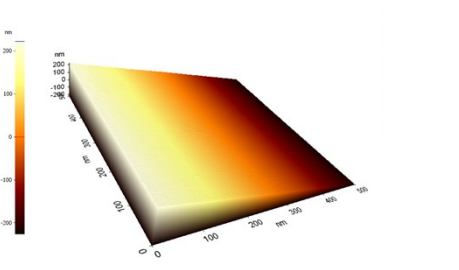
We have analysed the topography of the different PDMS surfaces using a combination of techniques. For determination of the topographic features dimension (depth/height (d_f/h_f) and width (w_f)) we have analysed the section profiles obtained from confocal reconstruction, and evaluated the quantitative data using ImageJ software. The results presented in Table S3 show that the different features had equivalent depth/height and width dimensions. We have also performed white light interferometry and atomic force macroscopy to analyse surface roughness at micro (Table S3) and nano-scale (Table S4). For AFM, we analysed $30 \times 30 \mu\text{m}^2$ and $3 \times 3 \mu\text{m}^2$ areas in various locations on the PDMS structures. In order to eliminate the influence of the macro-scale curvature of the surfaces on the roughness, we performed line by line fitting of the AFM data with second order polynomials. Smooth surfaces, with roughness values in the order of few nanometers (3-6 nm) were observed for all replicated samples (Table S4).

Table S3 Quantitative analysis of the surface topography. Dimensions of the topographic features were calculated from the cross-section profile obtained using confocal microscopy. Average sub-micro roughness of the different surface topographies were obtained by white light interferometry (Ambios Xi- 100) on 5 different areas of 1 mm^2 .

Structure	Confocal microscopy profiles		White light interferometry
	$d_f/h_f \pm \text{Std} (\mu\text{m})$	$w_f \pm \text{Std} (\mu\text{m})$	$Ra \pm \text{Std} (\mu\text{m})$
Dots	24.536 ± 0.385	11.629 ± 0.612	244 ± 14
Pits	24.042 ± 0.807	10.482 ± 0.779	241 ± 16
Cones	25.030 ± 0.428	10.599 ± 0.478	262 ± 27
Funnels	24.701 ± 0.534	10.598 ± 0.475	260 ± 22
Pyramids	24.125 ± 0.379	10.334 ± 0.233	403 ± 12
Inverted pyramids	24.800 ± 1.098	11.284 ± 0.461	362 ± 18

Table S4 . Examples of AFM images ($30 \times 30 \mu\text{m}^2$ and $3 \times 3 \mu\text{m}^2$) showing the surface roughness of different topographies.

Structure	Scan area $30 \times 30 \mu\text{m}^2$	Scan area $3 \times 3 \mu\text{m}^2$
Dots		

Pits		
Cones		
Funnels		
Pyramids	 <p data-bbox="375 1406 877 1471">Note: Lines represent a soft error due to height differences in scanning profile.</p>	
Inverted Pyramids		

References

1. D. Morrison and D. Jacobs, *Immunochemistry*, 1976, **13**, 813–818.
2. M. S. Cooperstock, *Antimicrob. Agents Chemother.*, 1974, **6**, 422–425.